

## *Electronic Supplementary Information*

### **Rare Earth Valve Manipulates Dual Regulation of Electronic States and Adsorption Geometry in the Selective Hydrogenation of Ethynylbenzene**

Kunhong Jiang, Yong Jiang, Zhong Liang, Wenshuo Zhang, Hengjun Liu, Jiali Shi, Siyuan Wang, Ziyun Zhong, Yaping Du\*

Tianjin Key Lab for Rare Earth Materials and Applications, Center for Rare Earth and Inorganic Functional Materials, School of Materials Science and Engineering, National Institute for Advanced Materials, Nankai University, Tianjin 300350, P. R. China

E-mail: ypdu@nankai.edu.cn

#### **Experimental section**

##### **Chemicals and materials**

Chloroplatinic acid hexahydrate ( $\text{H}_2\text{PtCl}_6 \cdot 6\text{H}_2\text{O}$ , 99.9%) was purchased from Adamas. Cobalt chloride hexahydrate ( $\text{CoCl}_2 \cdot 6\text{H}_2\text{O}$ , 99.99%) was purchased from Aladdin. Cerous chloride heptahydrate ( $\text{CeCl}_3 \cdot 7\text{H}_2\text{O}$ ) was obtained from Aladdin. 2-propanol ( $\text{C}_3\text{H}_8\text{O}$ , 99.9%) was purchased from Aladdin. Sulfuric acid ( $\text{H}_2\text{SO}_4$ ) and sodium (Na) were analytical purity and purchased from Tianjin Bohua. Carbon black (BP2000) was purchased from CABOT. Cyanamide ( $\text{CN}_2\text{H}_2$ , 99%) was purchased from Sigma-Aldrich. Ethynylbenzene ( $\text{C}_8\text{H}_6$ ), styrene ( $\text{C}_8\text{H}_8$ ), and ethylbenzene ( $\text{C}_8\text{H}_{10}$ ) were purchased from Admas-beta. Ammonia borane ( $\text{NH}_3\text{BH}_3$ , 97%) was purchased from Aladdin. n-dodecane ( $\text{C}_{12}\text{H}_{26}$ , 98%) was purchased from Heowns. *N,N*-dimethylformamide (DMF,  $\text{C}_3\text{H}_7\text{NO}$ , AR 99.5%), Methanol ( $\text{CH}_3\text{OH}$ , 99.9%), Dimethyl sulfoxide (DMSO,  $\text{C}_2\text{H}_6\text{OS}$ , 99.8%), Benzoic acid ( $\text{C}_7\text{H}_6\text{O}_2$ , AR 99.5%), Phenethyl alcohol ( $\text{C}_8\text{H}_{10}\text{O}$ , 99.5%), Acetonitrile ( $\text{CH}_3\text{CN}$ , 99.9%), Nitrobenzene ( $\text{C}_6\text{H}_5\text{NO}_2$ , 99%), and Aniline ( $\text{C}_6\text{H}_7\text{N}$ , AR 99%) were purchased from Aladdin. Benzaldehyde ( $\text{C}_7\text{H}_6\text{O}$ , 98%), Acetophenone ( $\text{C}_8\text{H}_8\text{O}$ , 98%), Benzyl alcohol ( $\text{C}_7\text{H}_8\text{O}$ , 98%),

4-Chlorobenzonitrile ( $C_7H_4ClN$ , 98%), and 4-Chlorobenzylamine ( $C_7H_8ClN$ , 98%) were purchased from Macklin. 1,4-Dioxane ( $C_4H_8O_2$ , 95%) Admas-beta. All of the reagents were analytical grade and used without further purification. Deionized water was used in all experiments.

### Synthesis of Catalysts

$Pt_{2-x}Co_xCe/C$  alloy was prepared by sodium vapor reduction. In the case of  $Pt_{1.5}Co_{0.5}Ce/C$  alloy, 16 mg  $H_2PtCl_6 \cdot 6H_2O$ , 3.6 mg  $CoCl_2 \cdot 6H_2O$  and 12 mg  $CeCl_3 \cdot 7H_2O$  were dissolved in 50 ml  $H_2O$ . 100 mg carbon black was added to the solution and the mixture was ultrasound for 30 min, then stirred overnight. The resultant mixture was rotary evaporated and dried at 60 °C for 12 h to produce precursor powder. In glove box, the precursor was put in a round BN crucible, and put this crucible together with another BN crucible containing Na ingot into a cuboid BN crucible with a sealable lid. The cuboid BN crucible was placed in Muffle oven and heated at 600 °C for 2 h with 5 °C/min heating rate. When the temperature naturally dropped to room temperature, the sample was taken out glove box and washed with 2-propanol, ethyl alcohol and water in turn. Finally, the obtain sample was treated with 0.5 M  $H_2SO_4$  to remove the thulium oxide, then dried in vacuum oven at 60 °C for 12 h to achieve  $Pt_{1.5}Co_{0.5}Ce/C$  alloy.  $Pt/C$  were synthesized in the same way except that  $CoCl_2 \cdot 6H_2O$  and  $CeCl_3 \cdot 7H_2O$  were not added.  $Pt_2Ce/C$  alloys were synthesized in the same way except that  $CoCl_2 \cdot 6H_2O$  was not added.  $PtCo/C$  were synthesized in the same way except that  $CeCl_3 \cdot 7H_2O$  was not added.

### Characterizations

X-ray diffraction (XRD) patterns were obtained by a Rigaku Smart-lab X-ray diffractometer (Rigaku, Japan) with Cu  $K\alpha$  radiation ( $\lambda = 1.5406 \text{ \AA}$ , 20 mA and 40 kV) and a scanning speed of 5 °min<sup>-1</sup>. The transmission electron microscopy (TEM) images were taken by a JEM-2100 electron microscope (JEOL, Japan) with an acceleration voltage of 200 kV. Elemental analysis in the samples was detected by inductively coupled plasma optical emission spectroscopy (ICP-OES, Agilent 5110, America). The chemical states of elements in catalysts were performed by X-ray photoelectron spectroscopy (XPS, Thermo Scientific ESCALAB

250Xi). The GC measurements of liquid samples were performed on Shimadzu GC 2010 Pro instrument equipped with a flame ionization detector and a WondaCap Wax capillary column (30 m × 0.25 mm). In situ DRIFTS characterization Diffuse reflectance infrared Fourier transform spectroscopy (DRIFTS) was performed on a Bruker INVENIO-R spectrometer, all spectroscopic tests were conducted at 4 cm<sup>-1</sup> spectral resolution. To obtain textural properties of catalysts, nitrogen physisorption was conducted with a Micromeritics ASAP2460 Automated Physisorption Instrument.

### **Catalyst evaluation:**

For ethynylbenzene hydrogenation reactions over pristine Pt/C and Pt<sub>2-x</sub>Co<sub>x</sub>Ce/C, EtOH (4.0 mL) and catalyst (3.0 mg) and reactant (1.0 mmol) were added into a 10 mL glass bottle equipped with a stir bar to form a uniform suspension under ultrasonic vibration. Then NH<sub>3</sub>-BH<sub>3</sub> (1.0 mmol, 30.9 mg) was added into the suspension. Prior to hydrogenation, the glass bottle was sealed and purged with argon gas for three times. Afterwards, the mixture was heated at 50 °C for 5 h under stirring in oil bath. The samples were filtered and analyzed by a gas chromatograph with a flame ionization detector (FID). Turnover frequency (TOF) was calculated as: TOF = (number of ethynylbenzene converted) / (surface Pt atoms) / (reaction time, h), at the reaction time of 20 min.

### **DFT calculations**

We used the DFT as implemented in the Vienna Ab initio simulation package (VASP) in all calculations.<sup>[1]</sup> The exchange-correlation potential is described by using the generalized gradient approximation of Perdew-Burke-Ernzerhof (GGA-PBE).<sup>[2-3]</sup> The projector augmented-wave (PAW) method is employed to treat interactions between ion cores and valence electrons. The plane-wave cutoff energy was fixed to 450 eV. Given structural models were relaxed until the Hellmann–Feynman forces smaller than -0.02 eV/Å and the change in energy smaller than 10<sup>-5</sup> eV was attained. Grimme’s DFT-D3 methodology was used to describe the dispersion interactions among all the atoms in adsorption models.<sup>[4, 5]</sup> The Gamma-centered k-points samplings were set to 2 × 2 × 1 for model. The vacuum space

along the z-direction was set to be 14 Å

The Gibbs free energy change is defined as:

$$\Delta G = \Delta E + \Delta ZPE - T\Delta S$$

where  $\Delta E$  is the electronic energy calculated with VASP,  $\Delta ZPE$  and  $\Delta S$  are the zero-point energy difference and the entropy change between the products and reactants, respectively, and  $T$  is the temperature (298.15 K).

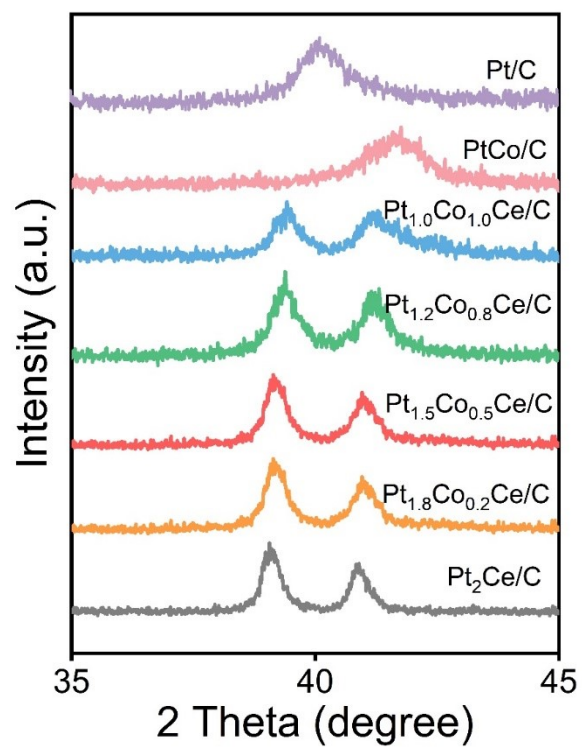


Figure S1 Enlarged XRD patterns of Pt<sub>2-x</sub>Co<sub>x</sub>Ce/C (x = 0, 0.2, 0.5, 0.8, 1.0).

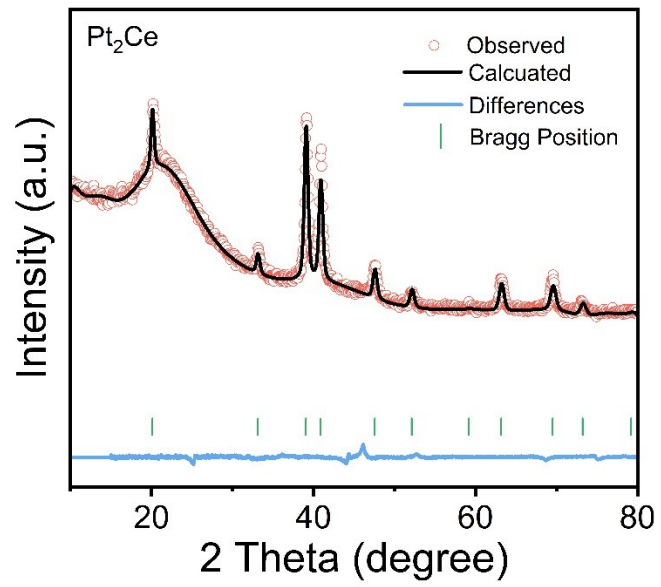


Figure S2 Rietveld refinement for the XRD pattern of Pt<sub>2</sub>Ce/C.

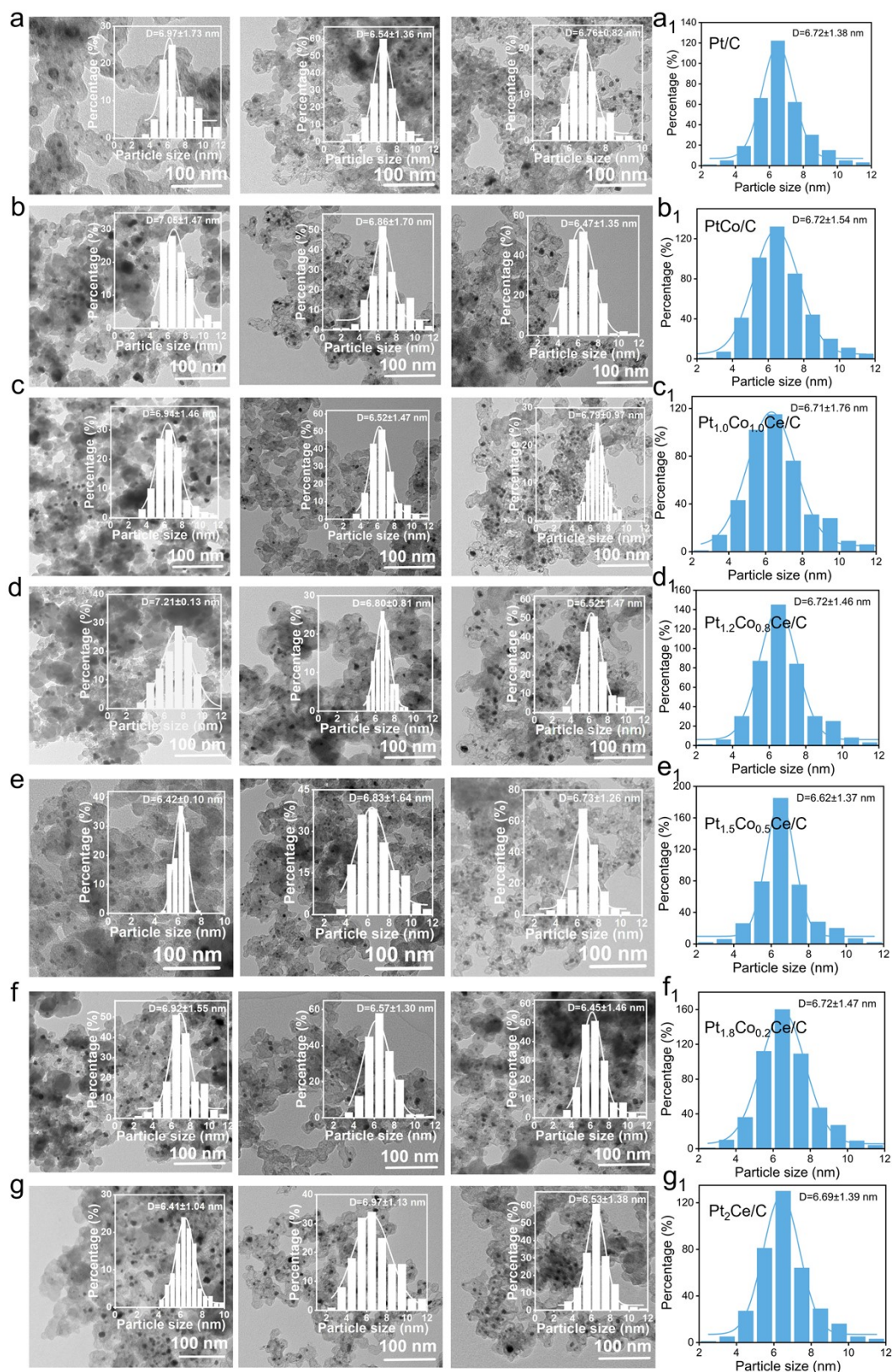


Figure S3 TEM images of (a) Pt/C, (b) PtCo/C, (c) Pt<sub>1.0</sub>Co<sub>1.0</sub>Ce/C, (d) Pt<sub>1.2</sub>Co<sub>0.8</sub>Ce/C, (e) Pt<sub>1.5</sub>Co<sub>0.5</sub>Ce/C, (f) Pt<sub>1.8</sub>Co<sub>0.2</sub>Ce/C, and (g) Pt<sub>2</sub>Ce/C. The insert is a statistical histogram of the size of the particles. (a<sub>1</sub>-g<sub>1</sub>) Average statistical analysis of particle sizes in multiple TEM images.

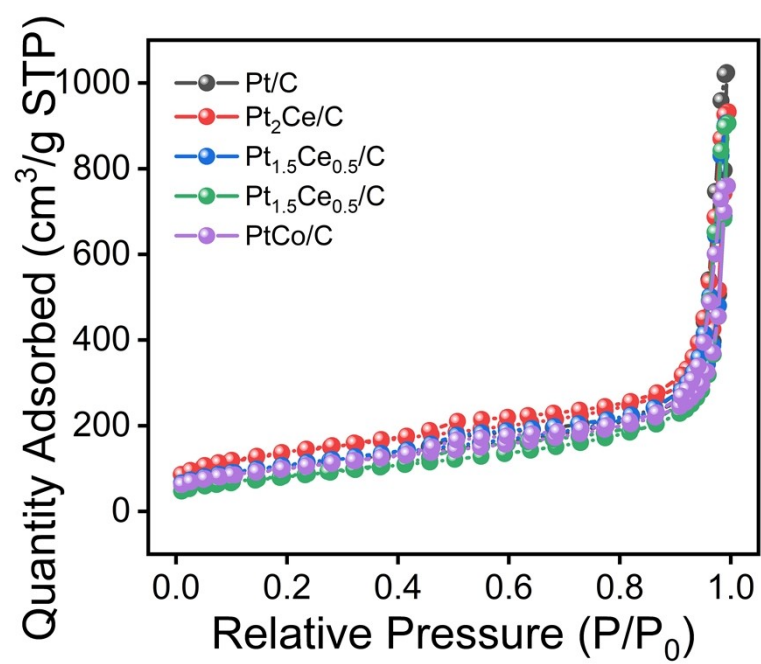


Figure S4 N<sub>2</sub> adsorption-desorption isotherms of samples.

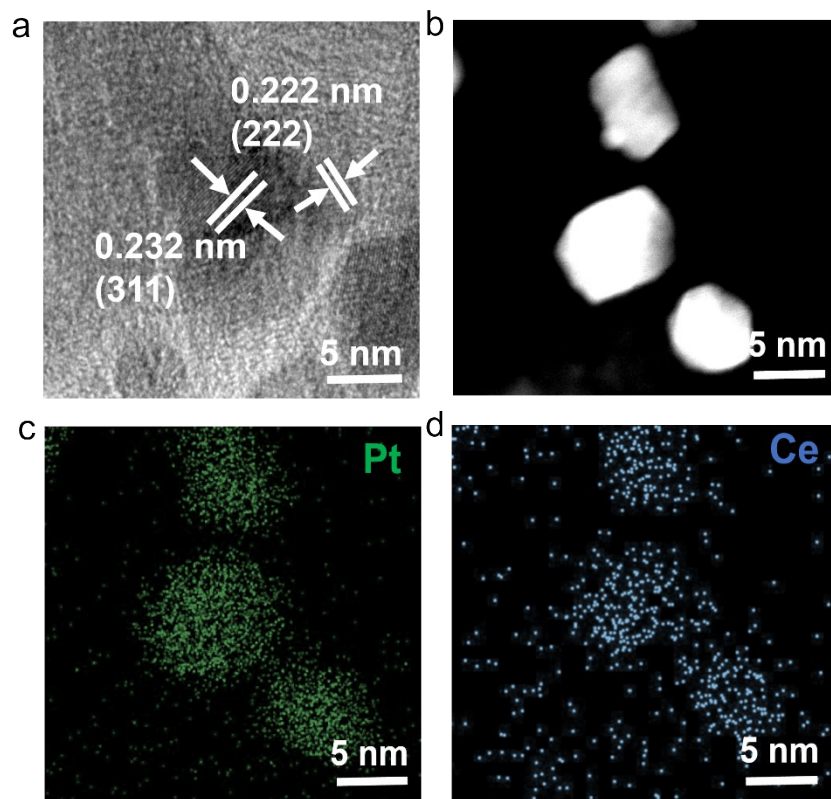


Figure S5 (a) HRTEM and (b-d) corresponding elemental mapping images of Pt<sub>2</sub>Ce/C.

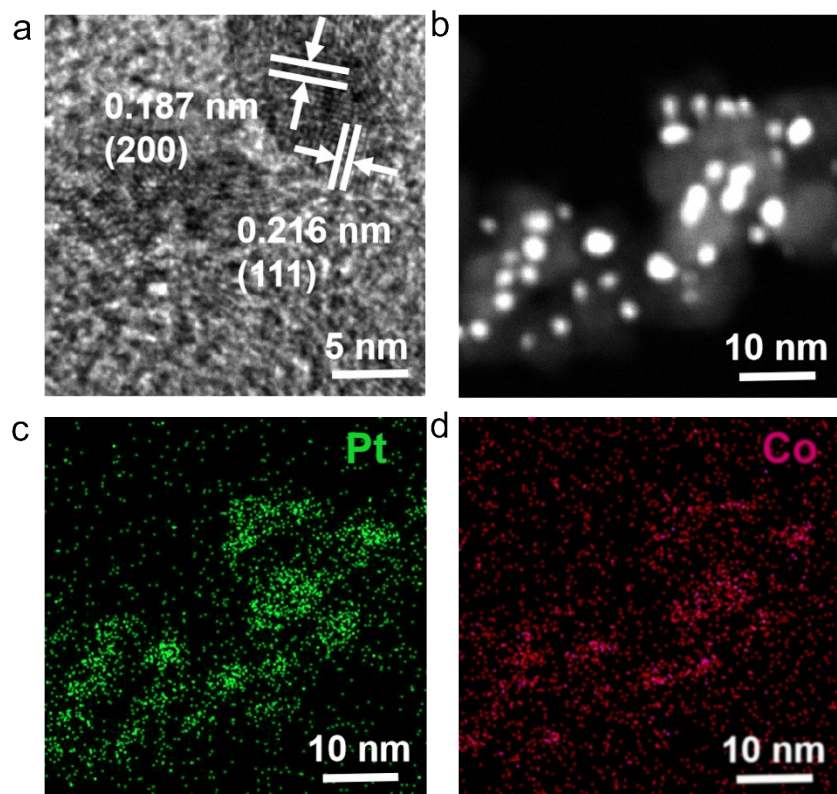


Figure S6 (a) HRTEM and (b-d) corresponding elemental mapping images of PtCo/C.

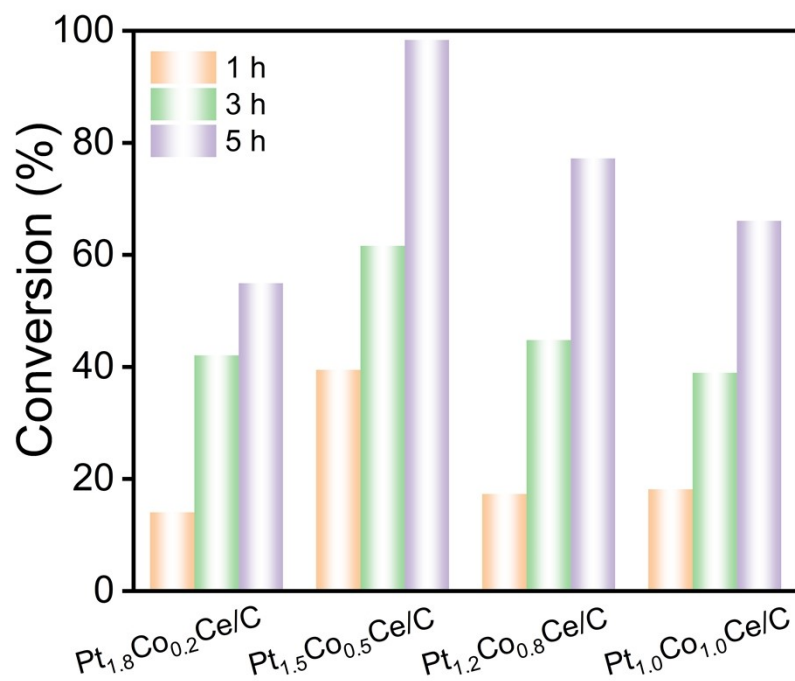


Figure S7 Catalytic performance of various  $\text{Pt}_{2-x}\text{Co}_x\text{Ce/C}$  catalysts in ethynylbenzene hydrogenation.

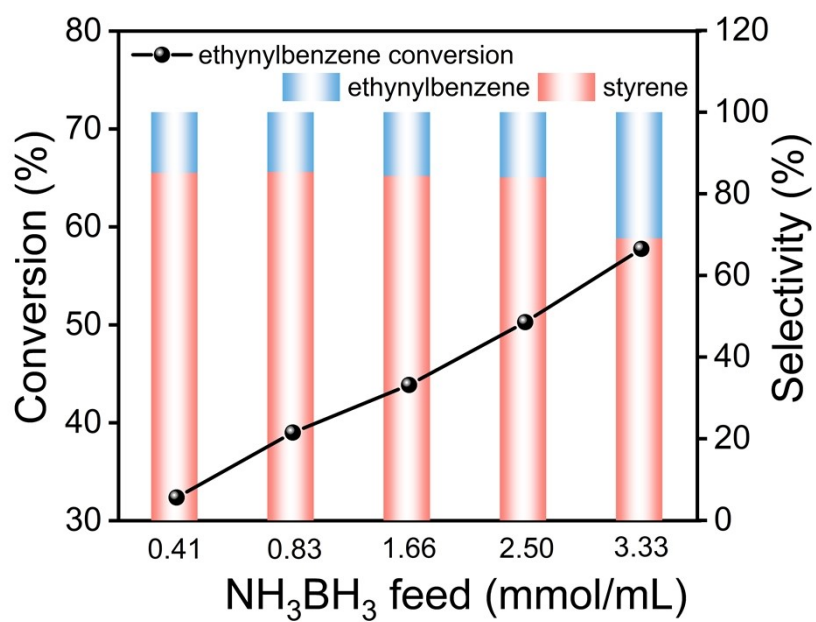


Figure S8 Ethynylbenzene hydrogenation performance in 1 h under different amounts of  $\text{NH}_3\text{BH}_3$  feed.

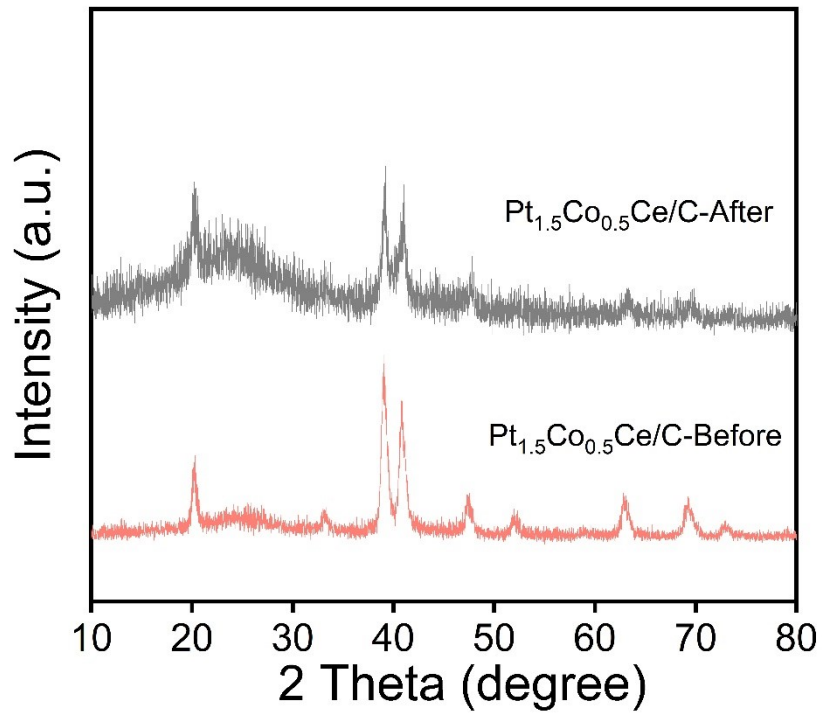
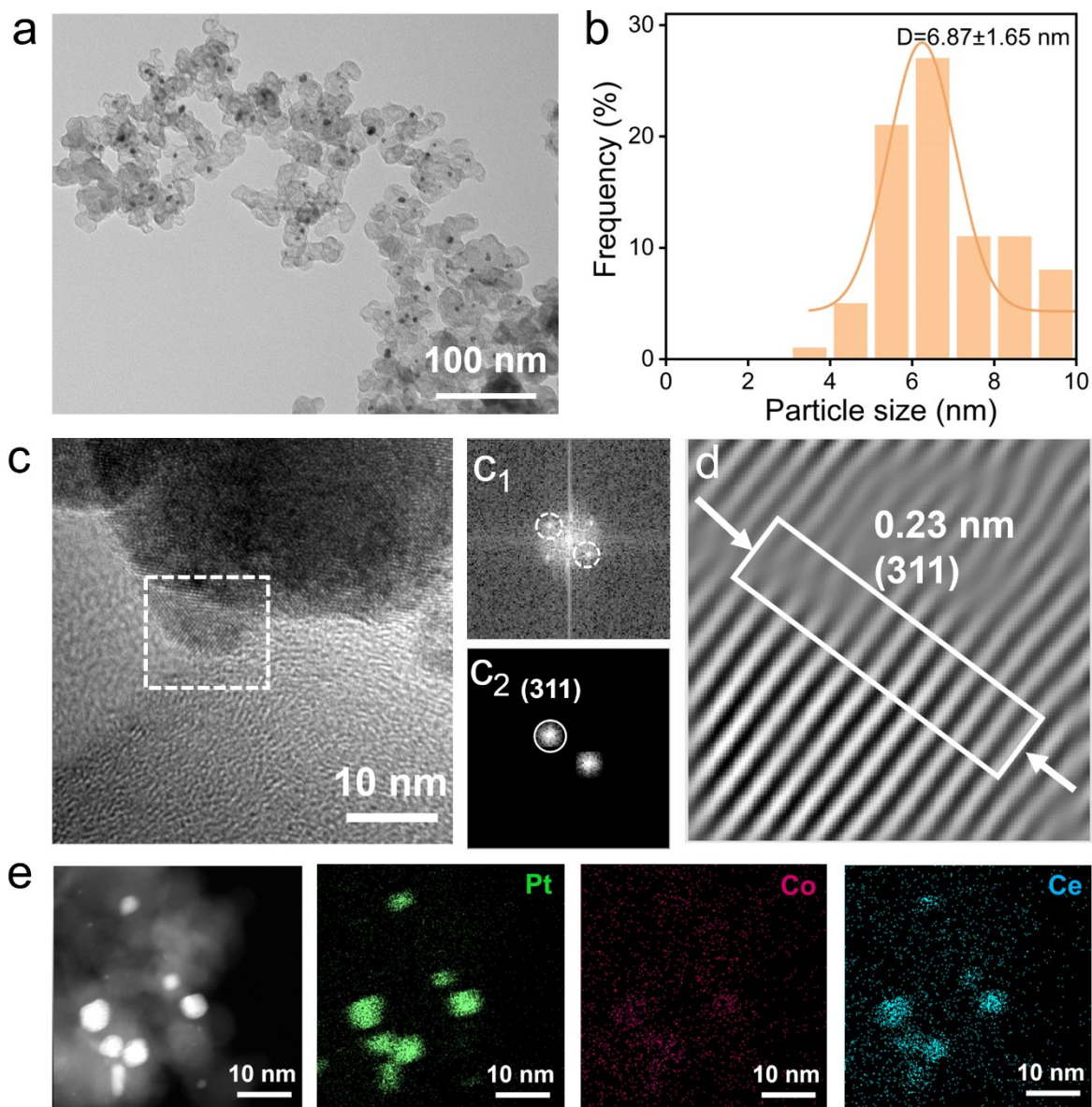


Figure S9 XRD patterns of Pt<sub>1.5</sub>Co<sub>0.5</sub>Ce/C before and after ten cycles.



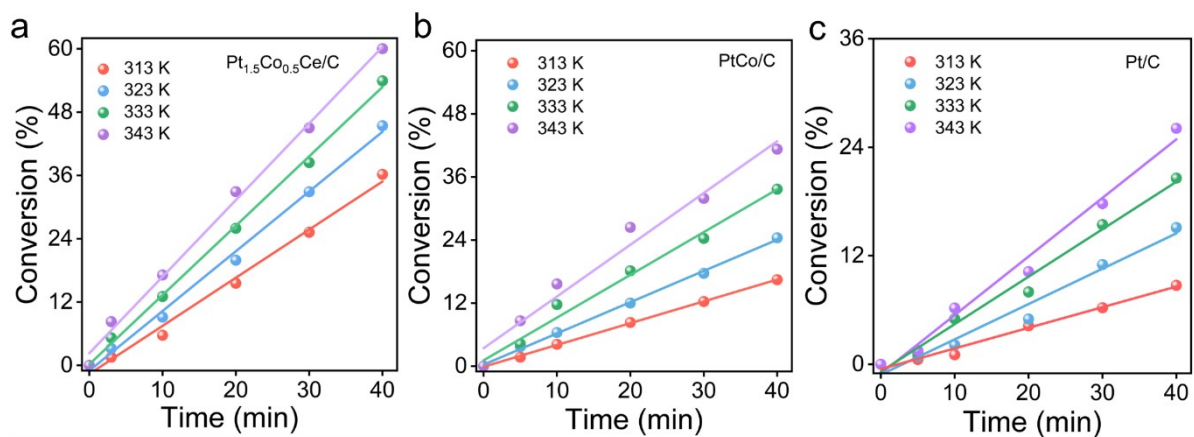


Figure S11 Effect of reaction temperature on ethynylbenzene hydrogenation conversion over (a) Pt<sub>1.5</sub>Co<sub>0.5</sub>Ce/C, (b) PtCo/C, and (c) Pt/C.

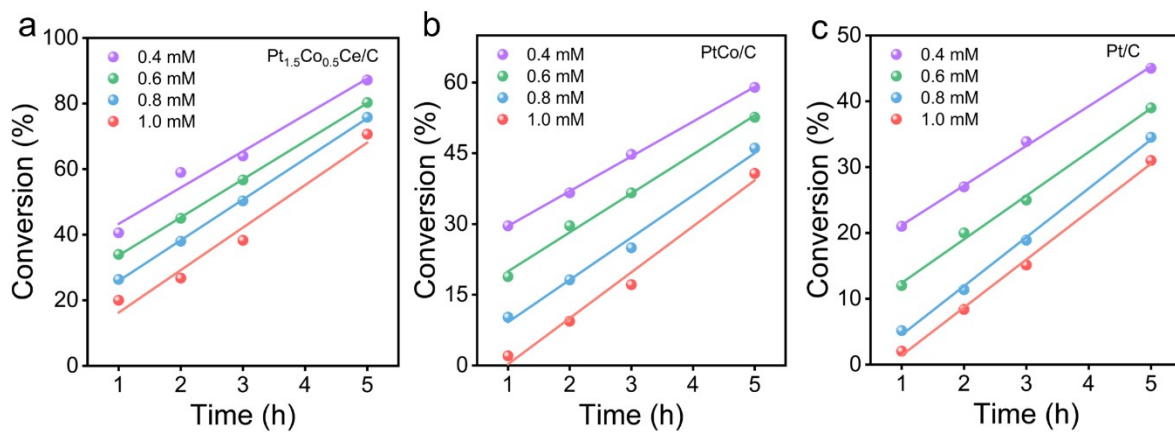


Figure S12 Effect of ethynylbenzene concentration on ethynylbenzene hydrogenation conversion over (a) Pt<sub>1.5</sub>Co<sub>0.5</sub>Ce/C, (b) PtCo/C, and (c) Pt/C.

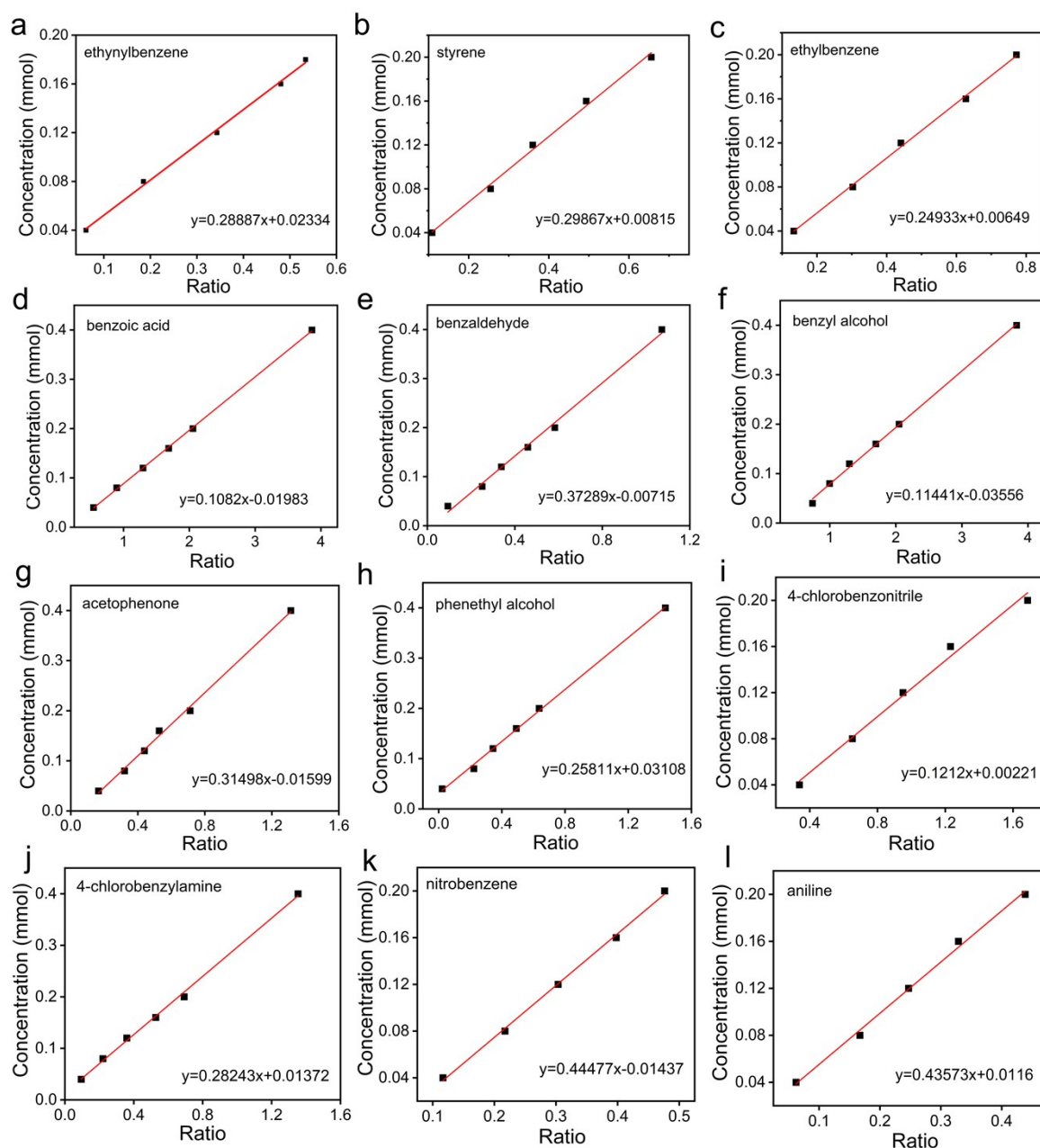


Figure S13 Calibration curves for various target compounds, (a) ethynylbenzene, (b) styrene, (c) ethylbenzene, (d) benzoic acid, (e) benzaldehyde, (f) benzyl alcohol, (g) acetophenone, (h) phenethyl alcohol, (i) 4-chlorobenzonitrile, (j) 4-chlorobenzylamine, (k) nitrobenzene, and (l) aniline.

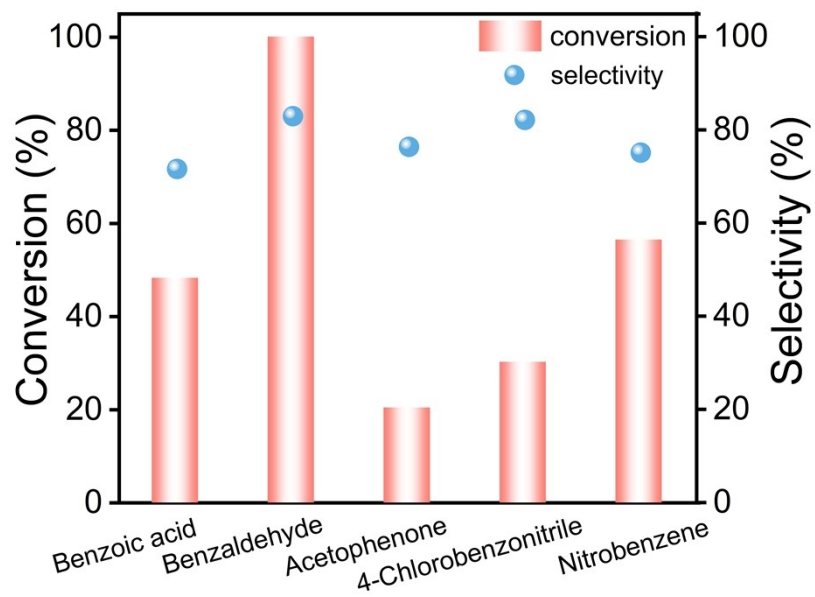


Figure S14 The performance of Pt<sub>1.5</sub>Co<sub>0.5</sub>Ce/C catalyst in the reduction of various functional groups.

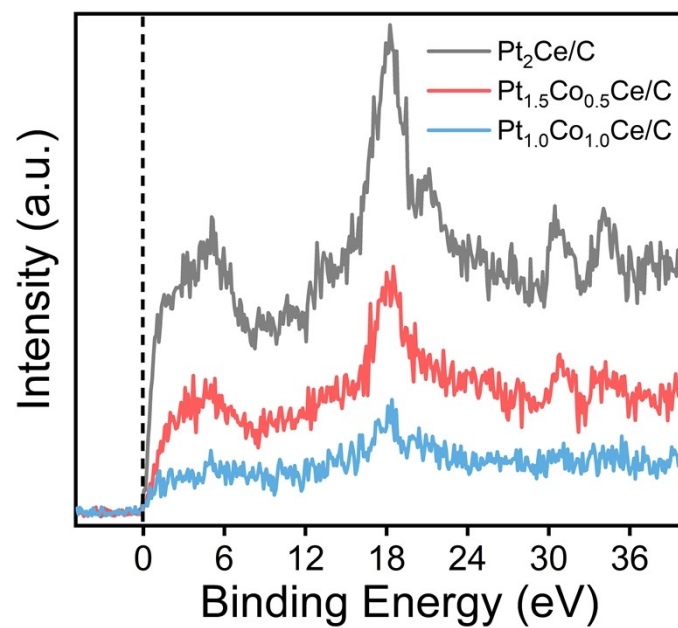


Figure S15 XPS valence band spectra of Pt<sub>2</sub>Ce/C, Pt<sub>1.5</sub>Co<sub>0.5</sub>Ce/C, and Pt<sub>1.0</sub>Co<sub>1.0</sub>Ce/C samples.

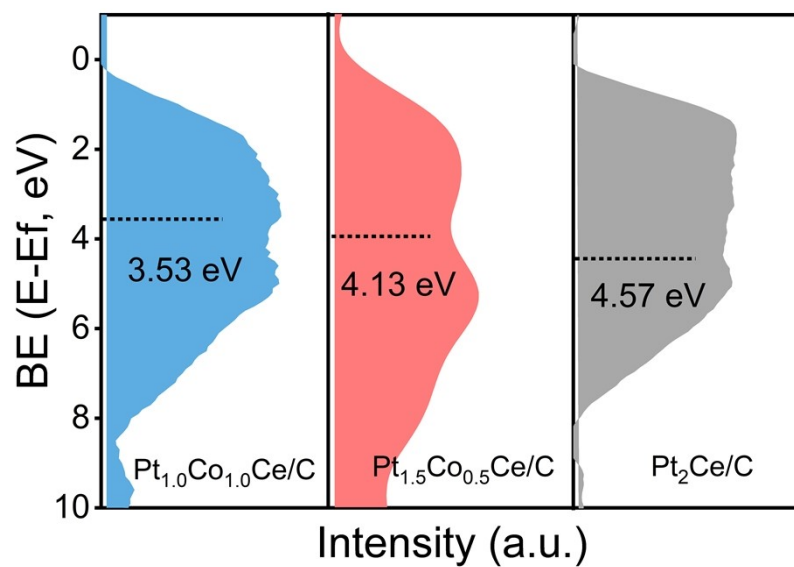


Figure S16 The d band center calculated from XPS valence band spectra of Pt<sub>2</sub>Ce/C, Pt<sub>1.5</sub>Co<sub>0.5</sub>Ce/C, and Pt<sub>1.0</sub>Co<sub>1.0</sub>Ce/C samples.

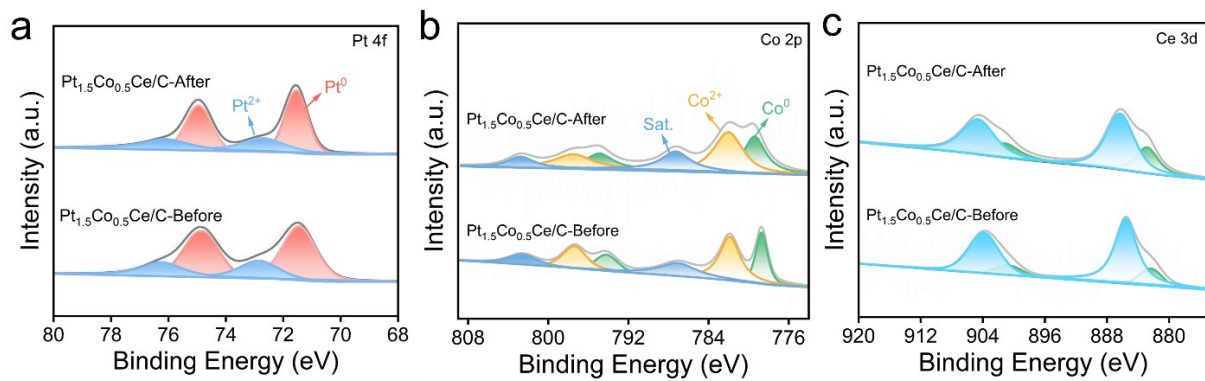


Figure S17 (a) Pt 4f, (b) Co 2p, and (c) Ce 3d XPS spectra of Pt<sub>1.5</sub>Co<sub>0.5</sub>Ce/C before and after cycles.

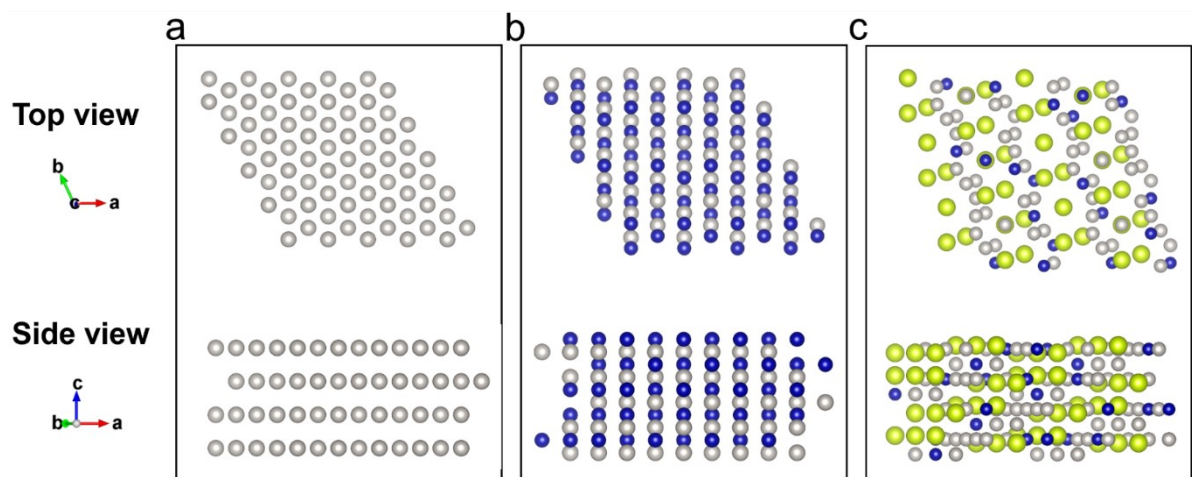


Figure S18 Schematic structures of the (a) Pt, (b) PtCo, and (c) PtCoCe models. The atoms in grey, blue, and yellow represent Pt, Co and Ce, respectively.

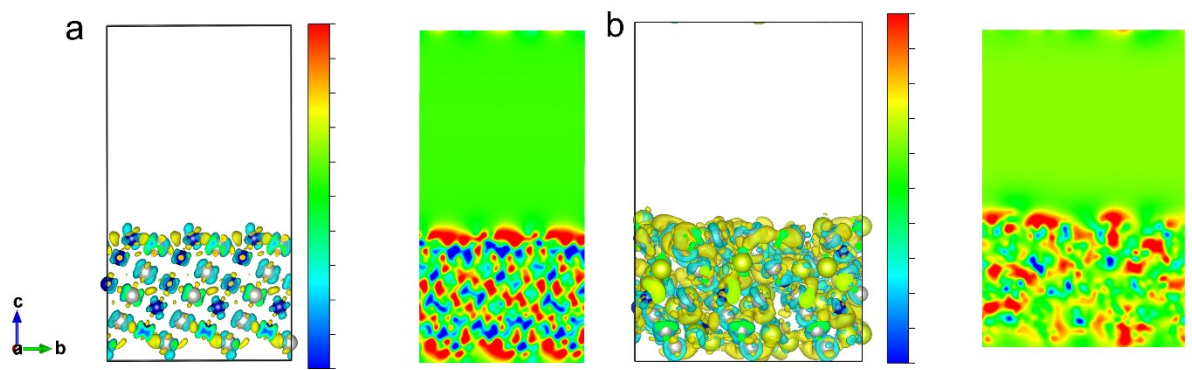


Figure S19 The charge density difference and contour maps of (a) PtCo/C, (b) Pt<sub>1.5</sub>Co<sub>0.5</sub>Ce/C.

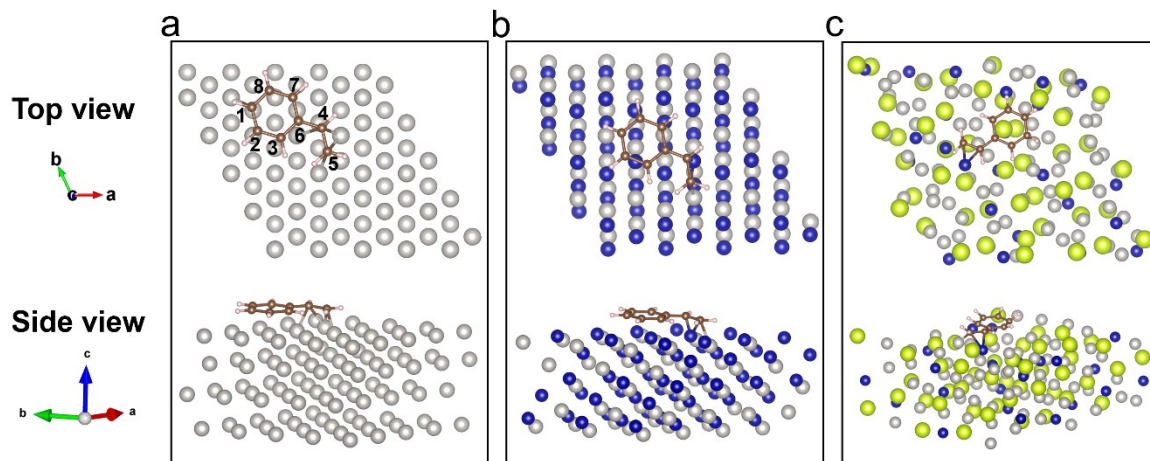


Figure S20 The adsorption configurations before optimized of styrene on the (a) Pt, (b) PtCo, and (c) PtCoCe models. The atoms in grey, blue, and yellow represent Pt, Co and Ce, respectively.

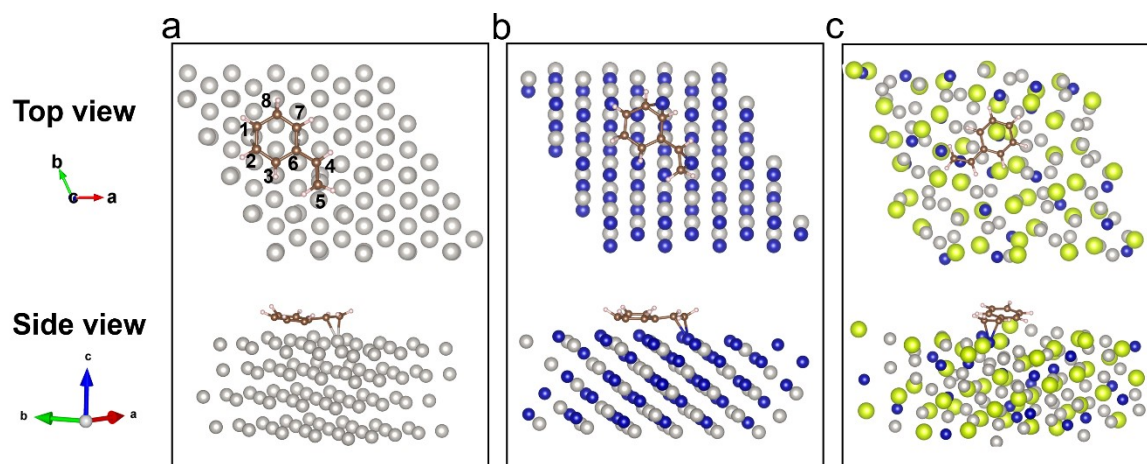


Figure S21 The adsorption configurations after optimized of styrene on the (a) Pt, (b) PtCo, and (c) PtCoCe models. The atoms in grey, blue, and yellow represent Pt, Co and Ce, respectively.

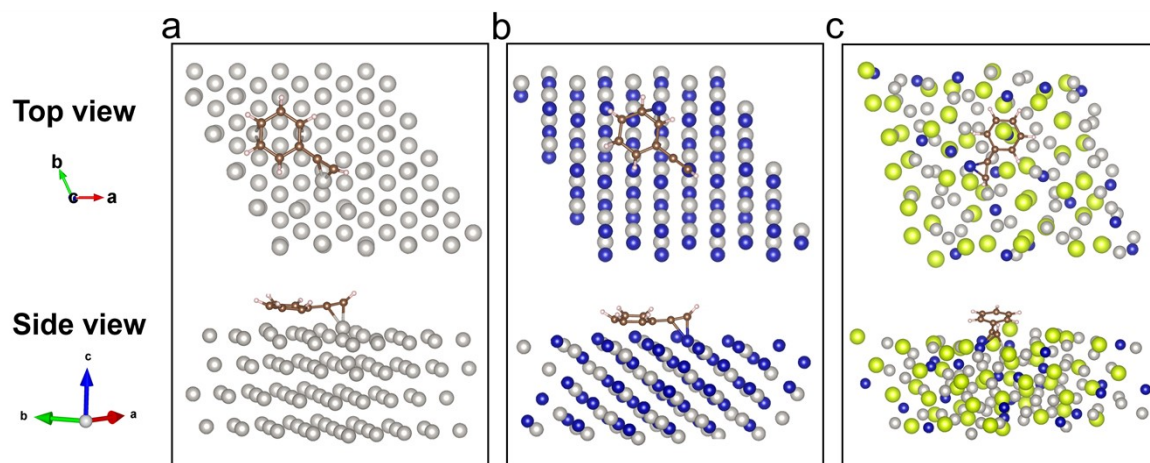


Figure S22 The adsorption configurations of ethynylbenzene on the (a) Pt, (b) PtCo, and (c) PtCoCe models. The atoms in grey, blue, and yellow represent Pt, Co and Ce, respectively.

Table S1 The ICP-OES results for samples.

Sample	Atomic ratio	Pt content (wt%)	Co content (wt%)	Ce content (wt%)
Pt/C	-	5.73	-	-
Pt <sub>2</sub> Ce/C	1.43 : 0.62	5.61	-	1.34
Pt <sub>1.5</sub> Co <sub>0.5</sub> Ce/C	1.33 : 0.25 : 0.51	5.21	0.10	1.51
PtCo/C	1.45 : 1.38	4.50	1.29	-

Table S2 Calculated results of crystal structure of Pt<sub>1.5</sub>Co<sub>0.5</sub>Ce/C based on Rietveld refinements of XRD patterns.

Sample	Pt <sub>1.5</sub> Co <sub>0.5</sub> Ce/C	Pt <sub>2</sub> Ce
Cell volume (Å <sup>3</sup> )	439.0	445.9
a=b=c	7.60	7.64
Pt–Ce/Co bond (Å)	3.166	3.167
Ce–Ce bond (Å)	5.400	5.402
R <sub>w</sub> (%)	1.97	4.15
GOF	1.22	0.93

Table S3 BET surface areas of samples.

Sample	BET surface area (m <sup>2</sup> /g)
Pt/C	373.20
Pt <sub>2</sub> Ce/C	350.53
Pt <sub>1.5</sub> Co <sub>0.5</sub> Ce/C	346.39
Pt <sub>1.0</sub> Co <sub>1.0</sub> Ce/C	329.72
PtCo/C	349.41

Table S4 Additional experiments of ethynylbenzene hydrogenation with Pt<sub>1.5</sub>Co<sub>0.5</sub>Ce/C.

Entry	Solvent	Reaction time (h)	Conversion (%)	Styrene sel. (%)
1	DMF	5 h	0.78	76.94
2	Methanol	5 h	0.43	83.03
3	Acetonitrile	5 h	0.40	86.55
4	Deionized water	5 h	77.11	12.15
5	EtOH:H <sub>2</sub> O (3:1)	5 h	86.54	76.61
6	EtOH:H <sub>2</sub> O (2:2)	5 h	99.90	5.14
7	DMSO	5 h	4.11	78.56
8	1,4-Dioxane	5 h	88.02	76.95

Table S5 Comparison of ethynylbenzene hydrogenation activity of the Pt<sub>1.5</sub>Co<sub>0.5</sub>Ce/C with the reported other Pt-based catalysts.

Catalyst	Reaction conditions	Activities	Ref.
Pt <sub>1.5</sub> Co <sub>0.5</sub> Ce/C		Con.=98%, Sel.=85%, TOF/h=1549	This work
PtCo/C	Ethynylbenzene(EB):Pt = 1000, 50°C, NH <sub>3</sub> BH <sub>3</sub> , 300 min	Con.=56%, Sel.=26%, TOF/h=640	This work
Pt <sub>2</sub> Ce/C		Con.=66%, Sel.=81%, TOF/h=769	This work
Pt/C		Con.=48%, Sel.=61%, TOF/h=379	This work
Pt@TS-1@TiO <sub>2</sub>	EB:Pt = 25, 30°C, 30 bar H <sub>2</sub> , 60 min	Con.=99%, Sel.=85%, TOF/h=191	[6]
Pt@UiO-66-F	EB:Pt = 150, 25°C, 10 bar H <sub>2</sub> , 45 min	Con.=98%, Sel.=55%, TOF/h=1500	[7]
Pt-Cd-700	EB:Pt = 320, 80°C, 4 bar H <sub>2</sub> , 240 min	Con.=99%, Sel.=86%, TOF/h=1828	[8]
Pt@X-zeolite	EB:Pt = 1464, 50°C, 5 bar H <sub>2</sub> , 360 min	Con.=95%, Sel.=81%, TOF/h=295	[9]
Pt <sub>1</sub> /CeO <sub>2</sub>	EB:Pt = 200, 30°C, 1 bar H <sub>2</sub> , 620 min	Con.=85%, Sel.=82%, TOF/h=163	[10]
Pt/C-0.5Cu	EB:Pt = 2000, 120°C, 60 bar H <sub>2</sub> , 180 min	Con.=100%, Sel.=94%, TOF/h=72	[11]
Pt@COF	EB:Pt = 1570, 25°C, 1 bar H <sub>2</sub> , 20 min	Con.=93%, Sel.=92%, TOF/h=3965	[12]
Pt <sub>0.2</sub> @ZSM-22	EB:Pt = 39, 65°C, 3 bar H <sub>2</sub> , 90 min	Con.=99%, Sel.=91%, TOF/h=5861	[13]
Pt <sub>1</sub> /PO <sub>4</sub> -CeO <sub>2</sub> -500	EB:Pt = 200, 60°C, 1 bar H <sub>2</sub> , 30 min	Con.=99%, Sel.=80%, TOF/h=316	[14]
Pt-Ni NF@CeO <sub>2</sub>	PA:Pt = 100, 50°C, 1 bar H <sub>2</sub> , 210 min	Con.=97%, Sel.=86%, TOF/h=187	[15]
CN@Pt/CNTs	EB:Pt = 1568, 50°C, 3 bar H <sub>2</sub> , 120 min	Con.=99%, Sel.=85%, TOF/h=1177	[16]
Pt/SiO <sub>2</sub>	EB:Pt = 100, 45°C, 20 bar H <sub>2</sub> , 40 min	Con.=42%, Sel.=88%, TOF/h=396	[17]
100TiO <sub>2</sub> /Pt/TiO <sub>2</sub>	EB:Pt = 251, 30°C, NH <sub>3</sub> BH <sub>3</sub> , 220 min	Con.=98%, Sel.=95%, TOF/h=232	[18]
Ru@Pt <sub>3</sub> /o-CNTs	EB:Pt = 1020, 50°C, 4 bar H <sub>2</sub> , 60 min	Con.=88%, Sel.=88%, TOF/h=191	[19]

Table S6 Catalytic performance of Pt<sub>1.5</sub>Co<sub>0.5</sub>Ce/C in the reduction of various functional groups.

Entry	Solvent	Conversion (%)	Selectivity (%)
1	Benzoic acid	48.25	Benzaldehyde 71.69
2	Benzaldehyde	100.00	Benzyl alcohol 83.03
3	Acetophenone	20.40	Phenethyl alcohol 76.45
4	4-Chlorobenzonitrile	30.21	4-Chlorobenzylamine 82.25
5	Nitrobenzene	56.42	Aniline 75.21

Reaction conditions: All reactions were carried out using 1.00 mmol substrate, 3.00 mg catalyst, 2.50 mmol/mL NH<sub>3</sub>BH<sub>3</sub>, 4.00 mL ethanol, at 50 °C for 5 h. Conversion and selectivity were determined by gas chromatography (GC) using n-dodecane as the internal standard.

Table S7 The change of configurational bond angle before and after optimization of adsorption of benzene ring in styrene over Pt, PtCo, and PtCoCe.

Bond angle (°)	Before adsorption optimized			After adsorption optimized		
	Pt	PtCo	PtCoCe	Pt	PtCo	PtCoCe
C <sub>8</sub> -C <sub>1</sub> -C <sub>2</sub>	120.00	120.02	121.72	121.72	118.68	119.60
C <sub>1</sub> -C <sub>2</sub> -C <sub>3</sub>	119.99	119.99	122.67	122.66	119.83	120.04
C <sub>2</sub> -C <sub>3</sub> -C <sub>6</sub>	119.99	119.98	116.24	116.26	119.55	121.36
C <sub>3</sub> -C <sub>6</sub> -C <sub>4</sub>	119.94	119.94	119.10	119.12	122.27	123.34
C <sub>6</sub> -C <sub>4</sub> -C <sub>5</sub>	119.76	119.76	123.85	125.59	127.48	124.25
C <sub>3</sub> -C <sub>6</sub> -C <sub>7</sub>	120.02	120.02	120.62	120.60	117.63	117.06
C <sub>6</sub> -C <sub>7</sub> -C <sub>8</sub>	119.98	119.98	123.00	123.00	121.11	121.65

Table S8 The change of configurational bond length and bond angle before and after optimization of styrene adsorption over Pt, PtCo, and PtCoCe.

Bond	Before adsorption optimized			After adsorption optimized		
	Pt	PtCo	PtCoCe	Pt	PtCo	PtCoCe
angle/length						
C <sub>6</sub> -C <sub>4</sub> -Pt (°)	53.497	49.371	90.640	47.454	52.796	75.093
C <sub>4</sub> -C <sub>5</sub> -Pt (°)	59.191	40.723	111.512	69.549	45.599	92.651
C <sub>6</sub> -C <sub>4</sub> (Å)	1.539	1.540	1.477	1.477	1.478	1.452
C <sub>4</sub> =C <sub>5</sub> (Å)	1.540	1.540	1.410	1.428	1.416	1.433
C <sub>5</sub> -Pt (Å)	2.170	2.166	1.944	2.107	3.236	3.568
C <sub>4</sub> -Pt (Å)	2.314	2.992	2.833	2.957	2.711	3.906
C <sub>6</sub> -Pt (Å)	1.867	2.307	3.209	2.240	2.165	3.801
C <sub>1</sub> -C <sub>6</sub> -Pt (°)	94.416	79.183	123.190	85.585	95.272	102.088

Table S9 Free energy for ethynylbenzene hydrogenation over Pt, PtCo, and PtCoCe.

Samples	Pt	PtCo	PtCoCe
C <sub>8</sub> H <sub>6</sub> Adsorption energy	-1.60	-1.77	-1.81
C <sub>8</sub> H <sub>7</sub> Free energy	-1.31	-0.60	-1.61
C <sub>8</sub> H <sub>7</sub> to C <sub>8</sub> H <sub>8</sub> Hydrogenation free energy	-0.57	-1.46	-0.65
C <sub>8</sub> H <sub>6</sub> to C <sub>8</sub> H <sub>8</sub> Hydrogenation free energy	-1.88	-2.06	-2.26
C <sub>8</sub> H <sub>8</sub> Adsorption energy	-0.83	-1.18	-0.33
C <sub>8</sub> H <sub>8</sub> to C <sub>8</sub> H <sub>9</sub> Hydrogenation free energy	-0.03	-0.29	+0.70
C <sub>8</sub> H <sub>8</sub> Desorption energy	+0.83	+1.18	+0.33
C <sub>8</sub> H <sub>9</sub> to C <sub>8</sub> H <sub>10</sub> Hydrogenation free energy	+0.01	-0.18	-

## References

1. G. Kresse, J. Furthmüller, *Phys. Rev. B.*, 1996, **54**, 11169.
2. J. P. Perdew, K. Burke, M. Ernzerhof, *Phys. Rev. Lett.*, 1996, **77**, 3865.
3. M. Ernzerhof, G. E. Scuseria, *J Chem Phys.*, 1999, **110**, 5029.
4. S. Grimme, J. Antony, S. Ehrlich, *J Chem Phys.*, 2010, **132**, 154104.
5. S. Grimme, S. Ehrlich, L. Goerigk, *J. Comput. Chem.*, 2011, **32**, 1456.
6. D. Gao, S. Wang, Y. Lv, C. Wang, J. Ren, P. Zheng, L. Song, A. Duan, X. Wang, G. Chen, C. Xu, *ACS Catal.*, 2024, **14**, 1939.
7. M. Guo, F. Wang, M. Zhang, L. Wang, X. Zhang, G. Li, *J. Catal.*, 2023, **424**, 221.
8. Y. Jin, P. Wang, X. Mao, S. Liu, L. Li, L. Wang, Q. Shao, Y. Xu, X. Huang, *Angew. Chem. Int. Ed.*, 2021, **60**, 17430.
9. Z. Zhang, G. Liu, L. Ding, M. Hu, J. Gu, W. Xu, Q. Xiao, *Inorg. Chem.*, 2021, **60**, 19120.
10. Y. Ma, X. Zhang, L. Cao, J. Lu, *Catal. Sci. Technol.*, 2021, **11**, 2844.
11. Y. Liu, W. Guo, X. Li, P. Jiang, N. Zhang, M. Liang, *ACS Appl. Nano Mater.*, 2021, **4**, 5292.
12. J. Li, Z. Yu, J. Li, Y. Fan, Z. Gao, J. Xiong, Li. Wang, Y. Tao, Y. Xiao, F. Luo, *J. Solid State Chem.*, 2020, **285**, 121176.
13. J. Tang, P. Liu, X. Liu, L. Chen, H. Wen, Y. Zhou, J. Wang, *ACS Appl. Mater. Inter.*, 2020, **12**, 11522.
14. Y. Ma, B. Chi, W. Liu, L. Cao, Y. Lin, X. Zhang, X. Ye, S. Wei, J. Lu, *ACS Catal.*, 2019, **9**, 8404.
15. Y. Long, J. Li, L. Wu, Q. Wang, Y. Liu, X. Wang, S. Song, H. Zhang, *Nano Res.*, 2019, **12**, 869.
16. L. Xia, D. Li, J. Long, F. Huang, L. Yang, Y. Guo, Z. Jia, J. Xiao, H. Liu, *Carbon* 2019, **145**, 47.
17. S. Jayakumar, A. Modak, M. Guo, H. Li, X. Hu, Q. Yang, *Chem. Eur. J.*, 2017, **23**, 7791.
18. H. Liang, B. Zhang, H. Ge, X. Gu, S. Zhang, Y. Qin, *ACS Catal.*, 2017, **7**, 6567.
19. C. Li, Z. Shao, M. Pang, C. T. Williams, X. Zhang, C. Liang, *Ind. Eng. Chem. Res.*, 2012, **51**, 4934.